Eur J Appl Physiol (2003) 90: 144–153
DOI 10.1007/s00421-003-0849-8

ORIGINAL ARTICLE

K. B. Geronilla · G. R. Miller · K. F. Mowrey · J. Z. Wu
M. L. Kashon · K. Brumbaugh · J. Reynolds · A. Hubbs
R. G. Cutlip

Dynamic force responses of skeletal muscle during stretch–shortening cycles

Accepted: 24 March 2003 / Published online: 9 July 2003

Abstract Muscle damage due to stretch–shortening cycles (i.e., cyclic eccentric/concentric muscle actions) is one of the major concerns in sports and occupational related activities. Mechanical responses of whole muscle have been associated with damage in neural motor units, in connective tissues, and the force generation mechanism. The objective of this study was to introduce a new method to quantify the real-time changes in skeletal muscle forces of rats during injurious stretch–shortening cycles. Male Sprague Dawley rats ($n = 24$) were selected for use in this study. The dorsi flexor muscle group was exposed to either 150 stretch–shortening cycles ($n = 12$) or 15 isometric contractions ($n = 12$) in vivo using a dynamometer and electrical stimulation. Muscle damage after exposure to stretch–shortening cycles was verified by the non-recoverable force deficit at 48 h and the presence of myofiber necrosis. Variations of the dynamic forces during stretch–shortening cycles were analyzed by decomposing the dynamic force signature into peak force (F_{peak}), minimum force (F_{min}), average force (F_{mean}), and cyclic force (F_a). After the 15th set of stretch–shortening cycles, the decrease in the stretch–shortening parameters, F_{peak}, F_{min}, F_{mean}, and F_a, was 50% ($P < 0.0001$), 26% ($P = 0.0055$), 68% ($P < 0.0001$), and 50% ($P < 0.0001$), respectively. Our results showed that both isometric contractions and stretch–shortening cycles induce a reduction in the isometric force. However, the force reduction induced by isometric contractions fully recovered after a break of 48 h while that induced by stretch–shortening cycles did not. Histopathologic assessment of the tibialis anterior exposed to stretch–shortening cycles showed significant myofiber degeneration and necrosis with associated inflammation, while muscles exposed to isometric contractions showed no myofiber degeneration and necrosis, and limited inflammation. Our results suggest that muscle damage can be identified by the non-recoverable isometric force decrement and also by the variations in the dynamic force signature during stretch–shortening cycles.

Keywords Muscle injury · Stretch–shortening cycles · Isometric · Eccentric · Concentric contractions

K. B. Geronilla · G. R. Miller · K. F. Mowrey · J. Z. Wu
M. L. Kashon · K. Brumbaugh · J. Reynolds · A. Hubbs
R. G. Cutlip (✉)
Engineering and Control Technology Branch,
National Institute for Occupational Safety and Health,
Morgantown, WV 26505, USA
E-mail: rgc8@cdc.gov
Tel.: +1-304-2855968
Fax: +1-304-2856265

Introduction

Traditionally, skeletal muscle injury has been studied using eccentric-only muscle actions where the muscle of interest is activated during the lengthening phase only (McCully and Faulkner 1986; Lieber et al. 1991; Warren et al. 1993). However, in voluntary activity, eccentric contractions occur during a stretch–shortening cycle. Thus, eccentric-only studies may not be as physiologically representative as studies involving stretch–shortening cycles. Muscle damage during stretch–shortening cycles is one of the major concerns in sports- and occupational-related activities. While there is evidence that muscle damage occurs during stretch–shortening exercise in humans (Kyrolainen et al. 1998) and animals (Stevens 1996), the majority of studies involving stretch–shortening cycles did not investigate muscle injury (Josephson 1985; Benn et al. 1998; Avela and Komi 1998).

While there is a paucity of studies that investigate stretch–shortening cycle-induced injury, there have been numerous studies of eccentric-contraction induced muscle injury (Morgan and Allen 1999). Studies using humans have demonstrated that repeated, intense, unaccustomed eccentric contractions result in myofibrillar ultrastructural disturbances immediately after the activity (Friden et al. 1983; Newham et al. 1983), delayed onset muscle soreness (Friden et al. 1981; Newham et al. 1987), and long-lasting muscle fatigue (Clarkson

and Newham 1995). Animal studies utilizing dynamometry techniques have been used to investigate the effect of exposure to unaccustomed eccentric contractions on mice (Faulkner et al. 1981; McCully and Faulkner 1986; Warren et al. 1993, 1996), rabbits (Lieber et al. 1991, 1996; Koh and Herzog 1998; Patel et al. 1998), and rats (Hesselink et al. 1996; Komulainen et al. 1998; Willems and Stauber 2000a, 2001). Studies using animals have shown that there is immediate post-exposure ultrastructural disorganization (Lieber et al. 1991), myofiber necrosis 1–3 days after exposure (McCully and Faulkner 1986; Lowe et al. 1995; Lieber et al. 1996; Hesselink et al. 1996; Komulainen et al. 1998), and a long-lasting force decrement (Ingalls et al. 1998). Considerable effort has been made to identify the parameters such as force, fiber strain, and strain rate that result in the immediate myofiber disruption and the subsequent long-lasting force decrement.

The effect of eccentric muscle actions on mechanical performance has been quantified by: (1) change in maximum isometric force or torque (Hesselink et al. 1996; Willems and Stauber 2001), (2) the isometric force deficit after each stretch (Willems and Stauber 2000b), (3) the change in peak force and force relaxation after each stretch (Willems and Stauber 2000a), and (4) the change in stiffness (Benz et al. 1998). However, eccentric-only studies to date have not measured in real-time (1) the decay in peak eccentric forces, (2) the change in magnitude and decay of isometric force preceding each stretch, (3) the decay in force enhancement during stretches, and (4) correlational analyses to determine if changes in real-time forces were predictive of myofiber damage.

There are some intrinsic benefits to investigating stretch–shortening exercise in the context of muscle damage that cannot be addressed by eccentric-only protocols. First, real-time changes in peak eccentric forces, isometric pre-test forces, and force enhancement during injurious stretch–shortening cycles can be quantified while the muscle is active. These changes in real-time parameters can allow for the detection of muscle damage occurrence in real-time and track the status of the muscle group of interest non-invasively. Second, synergistic effects of combined concentric and eccentric muscle actions can be studied in the context of resultant muscle damage and real-time changes in mechanical response. Third, this approach allows for more versatility in the temporal arrangement of sequential eccentric repetitions since the muscle is not deactivated during the concentric phase preceding each stretch. Thus, the effects of cycle frequency on real-time force response and muscle damage can be studied. Fourth, real-time changes in elastic and viscoelastic properties of muscle and the frequency dependence of these properties can be studied during cyclic loading. Fifth, this approach allows for the study of work loops and power absorption and generation in real-time and changes in those parameters during an injury-producing protocol. The work loop approach allows for the distinction between damage assessed as a decrease in positive work and power from damage assessed as a decrease in negative work and power.

As an initial step in elucidating muscle injury mechanisms during stretch–shortening cycles, the major purpose of the present study was to introduce a novel method to evaluate, in real-time, changes in force parameters during injurious stretch–shortening cycles. A custom-built dynamometer was used to control muscle contraction parameters and record muscle force produced during electrical stimulation of the dorsi flexor muscles in an in vivo rat model. In order to characterize the variations of the force parameters of the skeletal muscle during the stretch–shortening cycles, we evaluated the dynamic force responses of the muscle using four discrete representative mechanical properties: (a) peak eccentric forces, (b) magnitude of pre-stretch isometric forces, (c) magnitude of force enhancement, and (d) average forces during each stretch. The changes in magnitude and decay rate of these parameters associated with injurious stretch–shortening cycles have been quantified and are associated with contraction-induced damage. Muscle damage was operationally defined as a non-recovering isometric force decrement and the presence of myofiber necrosis 48 h after exposure to stretch–shortening cycles.

Methods

Male Sprague Dawley rats ($n = 24$) were selected for use in this study [mean (SD) 418 (13) g; 12 weeks of age]. All animals were housed in the animal quarters associated with the laboratory. Temperature and light–dark cycle were held constant for all animals; food and water were provided ad libitum. All animals were subjected to a standardized experimental protocol approved by the Animal Care and Use Committee of National Institute for Occupational Safety and Health before conducting the experimental protocols. Animals were randomly assigned to a stretch–shortening group ($n = 12$) or an isometric control group ($n = 12$).

Rats were tested on a custom-built rodent dynamometer (Cutlip et al. 1997) with improved software and data acquisition system. A Labview-based virtual instrument was developed that governs a data acquisition board (PCI-MIO-16XE-10, National Instruments) and a motion controller (Unidex 100, Aerotech Inc, Pittsburgh, Pa.) for precise control of a brushless DC servomotor (1410 DC, Aerotech) and muscle stimulator (Model SD9, Grass Medical Instruments, Quincy, Mass.). The software also acquires and stores experimental position, force, and velocity data described below.

Rats were anesthetized with isoflurane gas using a small animal anesthetic system (Surgivet Anesco). First, rats were placed in an "induction" tank filled with a mixture of isoflurane gas and oxygen; then, each rat was placed supine on the heated X–Y positioning table of the rodent dynamometer (Cutlip et al. 1997), with an anesthetic mask placed over its nose and mouth. The knee was secured in flexion (at 1.57 rad) with a knee holder. The left foot was secured in the load cell fixture with the ankle axis (assumed to be between the medial and lateral malleoli) aligned with the axis of rotation of the load cell fixture. Each animal was monitored during the protocol to ensure proper anesthetic depth and body temperature. The animal setup was similar to Willems and Stauber (1999).

The joint position of the ankle was defined by the angle between the tibia and the plantar surface of the foot. The angular position of the load cell fixture corresponds with angular position of the ankle. Vertical forces applied to an aluminum sleeve fitted over the dorsum of the foot were translated to a load cell transducer

(Sensotec) in the load cell fixture. The force produced by the dorsi flexor muscles was measured at the interface of the aluminum sleeve and the dorsum of the foot.

Platinum stimulating electrodes (catalogue no. F-E2, Grass Medical Instruments) were placed subcutaneously to span the peroneal nerve. Activation of the electrical stimulator resulted in muscle contraction of the dorsi flexor muscle group. Stimulator settings were optimized to maximize dorsi flexor contractile performance. Muscle stimulation for all protocols was conducted at 120 Hz stimulation frequency, 0.2 ms pulse duration, and 4 V in magnitude.

Isometric contractions were performed on the dorsi flexor muscle group 1 min before and after the exposure to either 15 sets of ten stretch–shortening cycles or 15 isometric contractions (Fig. 1) to evaluate the effect on force production. For the isometric pre- and post-test contractions, dorsi flexor muscles were stimulated for 1.0 s at an ankle angle of 1.57 rad. After a 48-h recovery interval, a second post-test was conducted.

The isometric control group was exposed to 15 contractions at 1 min intervals. During each contraction, dorsi flexor muscles were stimulated for 2.8 s at 1.57 rad using the same stimulation parameters as in the stretch–shortening group.

The stretch–shortening protocol that incorporated the isometric pre- and post-test contractions and stretch–shortening cycles was designed to quantify dorsi flexor force production in vivo under isometric (at 1.57 rad), concentric, and eccentric contractions. The stretch–shortening cycles were performed by fully activating the dorsi flexor muscles for 0.1 s and then moving the load cell fixture from 1.22 rad to 2.09 rad angular position at a velocity of 8.72 rad s^{-1}, in a reciprocal fashion, for ten oscillations and a duration of 2.4 s (allowing for motor ramp up and ramp down time) (Fig. 2A, B). Upon completion of ten oscillations, the load cell's motion terminated at 1.22 rad and the dorsi flexor group was deactivated 0.3 s after completion of the tenth oscillation for a total stimulation time of 2.8 s. The fifteen sets were also conducted at 1 min intervals.

Rats from both the isometric control group and stretch–shortening group were sacrificed either 30 min ($n = 12$) or 48 h ($n = 12$) after completion of the dynamometry exposure. Rats were weighed, anesthetized with sodium pentabarbital [IP, 10 mg (100 g body - weight)$^{-1}$], and exsanguinated. The left tibialis anterior muscle was dissected, cleaned, and weighed. The midbelly region was cut from

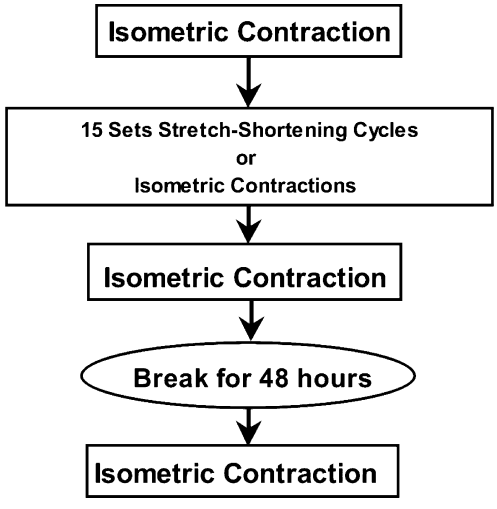

Fig. 1 Experimental procedure. In order to evaluate the mechanical property of the muscle in intact state, the dorsi flexor muscle group of the rats was contracted isometrically 2 minutes before the exposure to the stretch–shortening cycles. The stretch–shortening cycles consist of 15 exposures, each with ten lengthening/shortening cycles. Immediately after the stretch–shortening cycles, isometric contractions were conducted to evaluate the variations of the mechanical properties of the muscle. The final isometric contraction was conducted after a break of 48 h to evaluate the time-dependent muscle damage

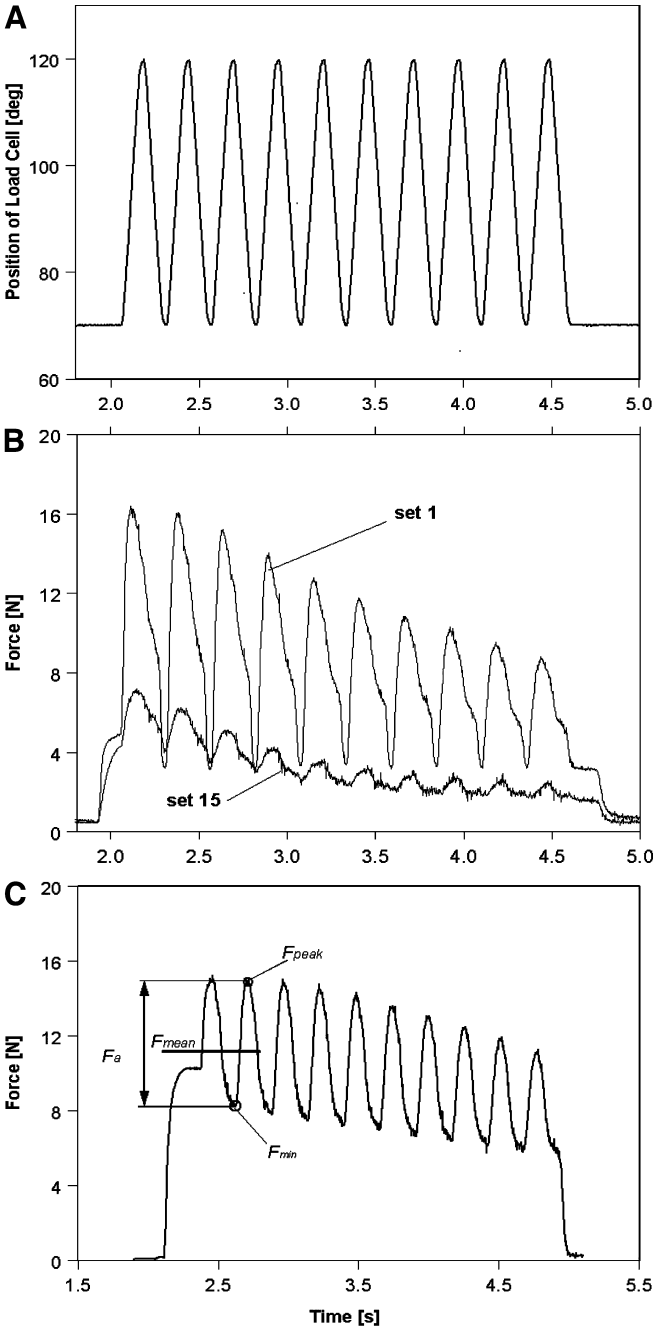

Fig. 2A–C Stretch–shortening cycles composed of 15 exposures, each with ten lengthening/shortening cycles. There was break of 1 min between two successive exposures. The muscle was fully activated during the stretch–shortening cycles. **A** Position–time history in each exposure. **B** Force responses of the muscle as a function of time for the first (set 1) and the last (set 15) exposures of stretch–shortening cycles. **C** Evaluation of the variations of mechanical properties of the muscle during the stretch–shortening cycles. The peak (F_{peak}), the minimum (F_{min}), the mean forces (F_{mean}), and the magnitude of cycling force (F_a) in each set of stretch–shortening cycles were evaluated

the muscle and mounted on cork, immersed in optimal cutting temperature medium (10.24% w/w polyvinyl alcohol, 4.26% w/w polyethylene glycol 85.50% w/w nonreactive ingredients), frozen in isopentane cooled with liquid nitrogen, and stored at −80°C until further use. Transverse sections (12 μm) were cut, mounted on pre-coated microscope slides, air dried, and stained using a routine procedure with Harris hematoxylin and eosin. Permount was used to attach coverslips to microscope slides. Tissue sections were evaluated on an Olympus BH-2 microscope. Digital pictures were obtained using an Olympus (Model AX70) microscope and a Quantix digital imaging system (Photometrics, Tucson, Ariz.). Morphologic assessment by a pathologist was selected for evaluation of the sections because it is an established method for evaluating muscle damage (Carter et al. 1998; Helliwell 1999) and because it allows assessment of injury across the entire muscle when swollen, atrophic, and necrotic fibers are all present in the same section. Frozen sections of tibialis anterior muscle were examined by a board-certified veterinary pathologist blinded to the exposure status of the rats. The distribution and severity of myositis and myofiber damage (degeneration and necrosis) were scored on a 5 point scale. Severity (intensity) was scored as minimal (1), mild (2), moderate (3), marked (4), or severe (5). Distribution (extent) was scored as focal (1), locally extensive (2), multifocal (3), multifocal and coalescent (4), or diffuse (5). The pathology score was calculated as the sum of the severity and distribution scores as previously described (Hubbs et al. 2002).

The experimental data for the 15 isometric contractions (isometric control, $n=6$) and 15 sets of stretch–shortening cycles (stretch–shortening group, $n=6$) were initially analyzed from the 12 animals sacrificed at 48 h and it was determined that sets 1, 3, 5, 7, and 15 represented the changes in mechanical behavior during the protocol. The data were processed to identify the parameters that characterize the mechanical responses of the dorsi flexor muscle group during repeated stretch–shortening cycles. The peak force (F_{peak}, defined as peak eccentric force), the minimum force (F_{min}, defined by the isometric force preceding each stretch), the average force (F_{mean}, obtained by calculating the average of muscle force values during the 100-ms eccentric phase of each oscillation), and the cyclic force ($F_a = F_{peak} - F_{min}$, defined by the force enhancement during each stretch) during the stretch–shortening cycles were evaluated, as illustrated in Fig. 2C. These parameters were quantified for the first oscillate in each set to determine changes between sets. Then, in order to evaluate the change in force parameters within each set, the repetition values for the peak, minimum, cyclic, and mean forces were fitted to an exponential curve:

$$F(t) = F_0 e^{-\alpha t}$$

where $F(t)$ and F_0 are the current and initial forces, respectively; t is the time (s); and α is the decay rate constant (1 s^{-1}). The decay rate constant represents the rate force parameters change within sets.

To determine whether the F_{min} values and decay rates during the stretch–shortening cycles were representative of fatigue, first the F_{min} values of sets 1, 3, 5, 7, and 15 were compared with the isometric forces in the control protocol at the corresponding time point and set of the F_{min} values. Second, the F_{min} decay rates of sets 1, 3, 5, 7, and 15 were compared with the decay rates of the isometric forces in the control protocol that were calculated in the same fashion as the decay rates of the stretch–shortening parameters.

Statistical analyses were conducted using SAS Version 8 (SAS Institute, Cary, N.C.), and were performed using the PROC MIXED procedure. Repeated measurement data were analyzed using the REPEATED option to model the within subjects covariance structure. Degrees of freedom were estimated using the Kenward-Roger method. Myofiber degeneration and necrosis scores and myositis pathology scores were analyzed by non-parametric Kruskal-Wallis test and all pair-wise comparisons were analyzed by Wilcoxon rank-sum test. Statistical significance was assessed at the 0.05 level.

Results

The maximum pre-test isometric forces of both the stretch–shortening and control groups were similar [11.43 (2.18) N and 9.58 (1.58) N respectively, $P=0.155$] and exhibited a similar reduction 2 min after the stretch–shortening cycles or isometric contractions [5.72 (0.68) N and 6.42 (0.68) N respectively, $P=0.255$]. However, it is interesting to observe that, 48 h after the exposure, the decreased isometric force of the control group exhibited a significant recovery from the 2-min value [10.38 (0.38), $P=0.0023$] thus resulting in full recovery, while the isometric forces from the stretch–shortening group remained depressed and showed no significant change [5.91 (0.68) N, $P=0.85$] (Fig. 3).

Tibialis anterior muscle sections from rats undergoing 3, 7, or 15 sets of ten stretch–shortening cycles, 15 sets of isometric contractions, and control (resting) rats were assessed by histopathologic evaluation of frozen sections at 48 h recovery (Fig. 4A–D). Myofiber degeneration and necrosis was not seen in control rats or rats undergoing isometric contractions (Fig. 4A). In contrast, muscles exposed to stretch–shortening cycles did result in myofiber degeneration and necrosis, particularly in those exposed to 70 stretch–shortening cycles (Fig. 4C) and 150 stretch–shortening cycles (Fig. 4D), but to a much lesser degree in those exposed to 30 stretch–shortening cycles (Fig. 4B). Morphologically, myofiber degeneration and necrosis was characterized by remarkable heterogeneity in myofiber diameter with myofiber swelling, hyalinization, atrophy, necrosis, and phagocytosis (Fig. 4C, D). The myofiber degeneration and necrosis was accompanied by interstitial edema and

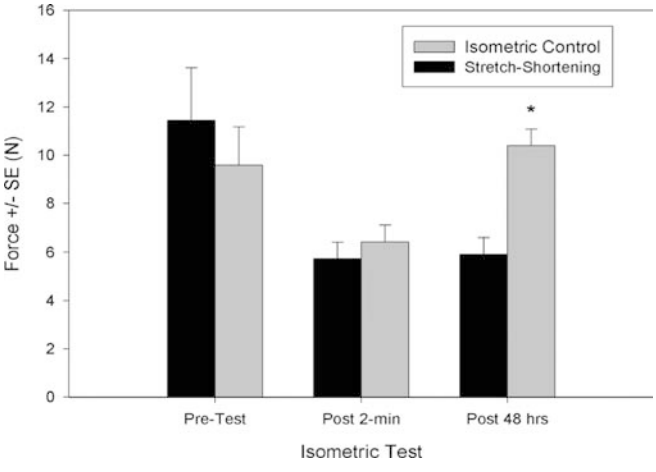

Fig. 3 Comparison of the isometric force after the exposure to the stretch–shortening cycles with that before the exposure to the stretch–shortening cycles. The labels *Pre-Test*, *Post 2-min*, and *Post 48 hrs* imply that the tests were conducted 2 min before, 2 min after, and 48 h after the exposures to the stretch–shortening cycles, respectively. Statistical analyses indicated that there was significant recovery of the isometric control group from Post 2-min to Post 48 hrs ($P=0.0023$) while the stretch–shortening group did not exhibit any change ($P=0.85$)

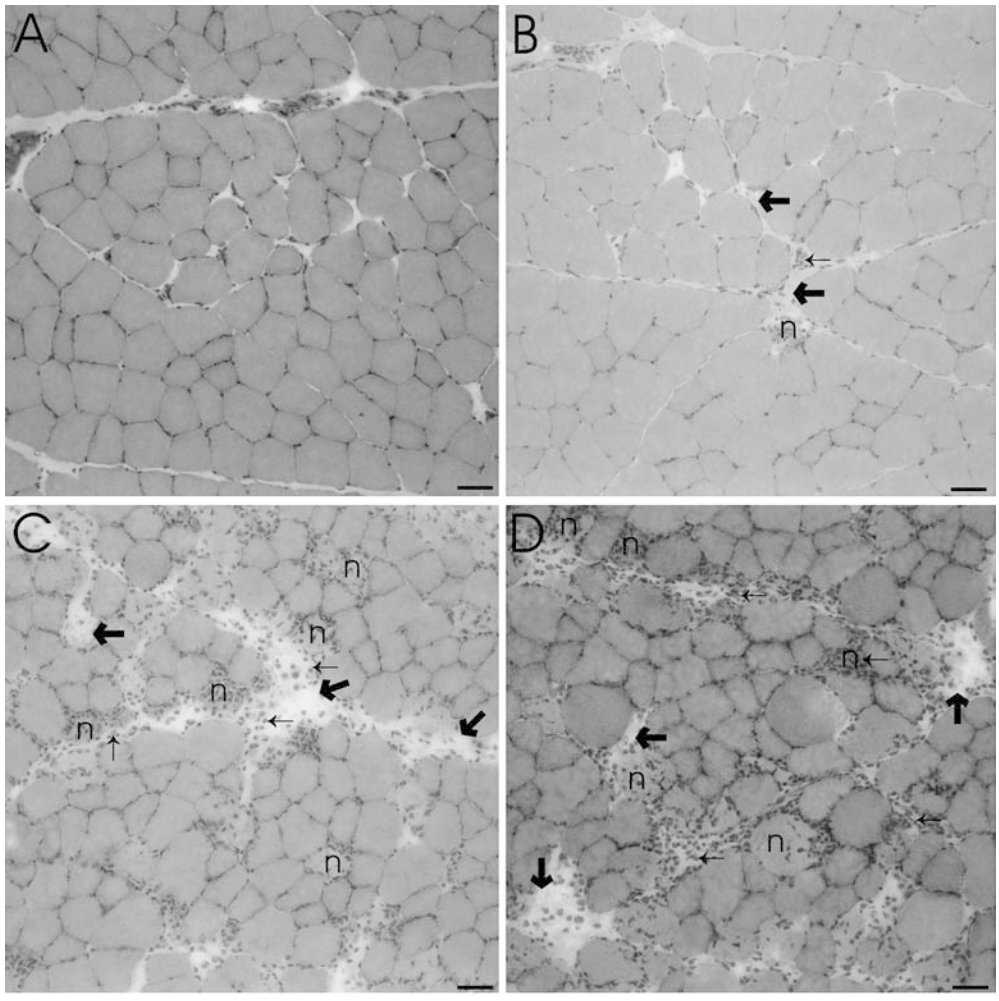

Fig. 4A–D Comparison of the structures of "injured" muscle with those of "uninjured" muscle. The histological pictures of the cross section of the dorsi flexor muscle of rats were taken using a magnification of ×40. **A** Thirty minutes after isometric contractions (control). **B** Forty-eight hours after 30 stretch–shortening cycles. **C** Forty-eight hours after 70 stretch–shortening cycles. **D** Forty-eight hours after 150 stretch–shortening cycles. The reference bar in the photomicrographs is 50 μm. Each *thick arrow* indicates edema, while each *thin arrow* indicates inflammation. *n* The observation of a necrotic myofiber

infiltration of inflammatory cells, features of myositis (Fig. 4C, D). Pathology scores for myofiber degeneration and necrosis increased with increasing numbers of stretch–shortening cycles, and were significantly greater than control values after 7 or 15 sets of stretch–shortening cycles ($P < 0.05$, Fig. 5A). Pathology scores for myositis (as assessed by inflammatory cell infiltrates) also increased with increasing numbers of stretch–shortening cycles ($P < 0.05$, Fig. 5B). To help identify the time course in the development of morphologic change in the tibialis anterior muscle, sections from rats undergoing 15 sets of ten stretch–shortening cycles or 15 isometric contractions were also assessed by histopathologic evaluation of frozen sections at 30 min recovery. In rats undergoing 150 stretch–shortening cycles, myofiber degeneration and necrosis (Fig. 5C) and myositis (Fig. 5D) at 48 h were significantly greater ($P < 0.05$) than observed after 30 min recovery. Exposure to 15 sets of isometric contractions resulted in limited inflammation but myositis severity after isometric contractions was never considered greater than mild 48 h after exposure (Fig. 5D).

The experimental data collected from the isometric control and stretch–shortening group were analyzed to determine if there were differences in mechanical behavior between the two groups that might explain the difference in isometric force recovery and histological response. First, the muscle force responses to stretch–shortening cycles as a function of time (Fig. 2B) are plotted together with the prescribed displacement history (Fig. 2A). A comparison of the force history for sets 1 and 15 of the stretch–shortening cycles indicates a dramatic decline in the magnitude of force levels (Fig. 2B). Also, the muscle force responses for the control group during the 15 isometric contractions showed a pronounced force decrement. The dynamic force response during the stretch–shortening cycles was then further evaluated by decomposing the force signature into representative F_{peak}, F_{min}, F_{mean}, and F_a (Fig. 2C).

These parameters were plotted as a function of the number of cycles for exposure sets 1, 3, 5, 7, and 15 (Fig. 6). The mean and SEM for these analyses are also indicated in Fig. 6. The variation in F_{min} (Fig. 6A) is small from set 1 to set 15 of stretch–shortening exposures. However, F_{mean} (Fig. 6B), F_{peak} (Fig. 6C), and F_a (Fig. 6D) declined with increasing sets, and the magnitude of these force parameters tend to decrease remarkably after several exposures to the stretch–shortening cycles.

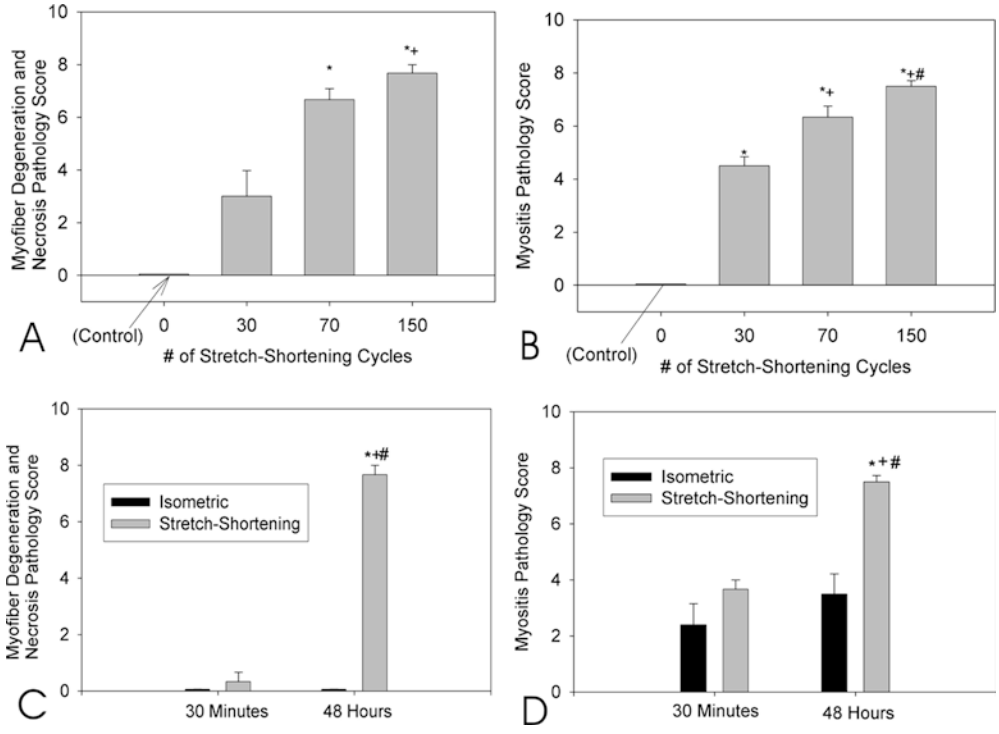

Fig. 5A–D Pathology scores for myofiber degeneration and necrosis. **A** Myofiber degeneration and necrosis pathology scores for the control muscles, and tibialis anterior muscles exposed to 30, 70, and 150 stretch–shortening cycles sampled 48 h after exposure. **B** Myositis pathology scores for the control muscles, and tibialis anterior muscles exposed to 30, 70, and 150 stretch–shortening cycles sampled 48 h after exposure. **C** Myofiber degeneration and necrosis pathology scores for the group exposed to 15 sets of isometric contractions and 15 sets of stretch–shortening contractions. Data are presented from tissue analyzed at 30 min and 48 h after exposure. **D** Myositis pathology scores for the group exposed to 15 sets of isometric contractions and 15 sets of stretch–shortening contractions. Data are presented from tissue analyzed at 30 min and 48 h after exposure. Data are presented as means (SEM) ($n = 6$ per group). In **A** and **B**, *, +, and # denote differences from control, 30 repetition, and 70 repetition groups, respectively. In **C** and **D**, *, +, and # denote differences from isometric at 30 min, stretch–shortening at 30 min, and isometric at 48 h, respectively. Significance is noted at the 0.05 level

The magnitude of F_a appears to stabilize after about seven exposures to the stretch–shortening cycles. The change in F_{peak}, F_{min}, F_{mean}, and F_a for sets 1, 3, 5, 7, and 15 was then quantified (Fig. 7A). The decrease in the stretch–shortening parameters, F_{peak}, F_{min}, F_{mean}, and F_a, from set 1 to set 15 was 50% ($P < 0.0001$), 26% ($P = 0.0055$), 68% ($P < 0.0001$), and 50% ($P < 0.0001$), respectively. The change in the force parameters between sets was subsequently analyzed to determine if changes were evident during the protocol.

There was a significant set effect for F_{peak} ($P < 0.0001$). Post hoc analysis indicated that there was a significant decline in F_{peak} occurring with each set as all pair-wise differences were significant. There was also a significant set effect for F_{min} ($P = 0.0003$), F_a ($P < 0.0001$), and F_{mean} ($P < 0.0001$). Further analysis indicated that the mean values of F_{min} at set 1 were significantly greater than those at sets 3, 5, 7, and 15 while remaining pair-wise differences were not significant. These results indicated that F_{min} did not exhibit a statistically different change from set 3 to set 15. In contrast, all pair-wise differences in the mean values of F_a were significant which indicated a continual decline from set 1 to set 15 (Fig. 7A). The F_{mean} values exhibited similar behavior to F_a since all pair-wise differences in the mean values were also statistically significant with the exception of set 5 and set 7, which were not statistically different ($P = 0.2606$).

The changes in force during the isometric control protocol were then analyzed for similarities to the stretch–shortening protocol. During the isometric control protocol, there was a 25% force decrement between sets 1 and 15 (Fig. 7B). The decrement for F_{min} during the stretch–shortening cycles was similar (approximately 30%). In addition, F_{min} values were compared to isometric forces in the control protocol that corresponded to the same time point (Fig. 7B). There was a significant effect with treatment ($P = 0.0330$) due to the difference in magnitude between the isometric control and F_{min} values. There was also a significant effect of set ($P < 0.0001$); however, there was no significant interaction between treatment and set ($P = 0.0940$). The non-significance of the treatment–set interaction indicated that the F_{min} values and isometric control values exhibited similar behavior during the 15 sets.

In order to determine the change in the force parameters within set during the 15 sets of stretch–shortening cycles, the α values of the force parameters F_{peak}, F_{min}, F_{mean}, and F_a were quantified (Fig. 8A). For set 1, α was approximately 0.03 ($1\ s^{-1}$) for all force parameters. There was a significant effect of set for α

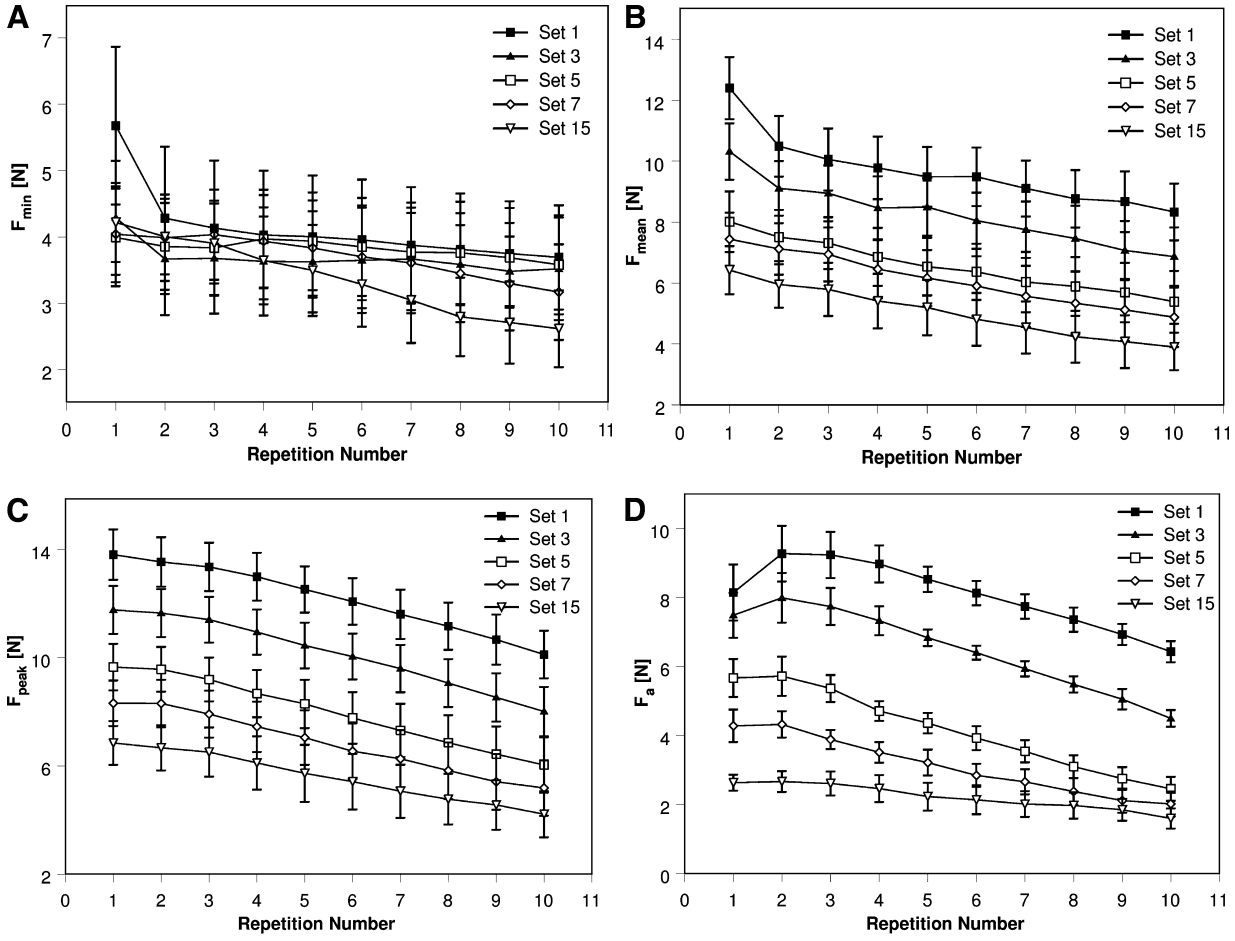

Fig. 6A–D The variation of the mechanical properties of the muscle during the stretch–shortening cycles. **A**, **B**, **C**, **D** The F_{min}, F_{mean}, F_{peak}, and F_a, respectively, as a function of the number of cycles

values for F_a ($P=0.0195$) and F_{min} ($P=0.002$) while α values for F_{peak} ($P=0.4848$) and F_{mean} ($P=0.5435$) did not exhibit a significant change with set (Fig. 8A). Post hoc analyses of α values for F_a indicated that set 5 ($P=0.0042$) and set 7 ($P=0.0054$) were significantly different than set 1 and all other pair-wise differences were not significant. This result indicated that α values for F_a did not increase after set 5. In contrast, α values for F_{min} increased during the protocol. Post hoc analyses indicated that set 15 was significantly different than set 1 ($P=0.0193$), set 3 ($P=0.0004$), set 5 ($P=0.0001$), and set 7 ($P=0.0009$), and set 7 was different than set 5 ($P=0.031$). It is interesting to note that the α values of all the force parameters are nearly equivalent by set 15 (Figure 8A). In order to determine whether the α values for F_{min} of the stretch–shortening group were representative of fatigue, those rates were compared with the isometric force α values in the control protocol (Fig. 8B). The results indicated that there was a significant main effect of set ($P<0.0001$), but there was no effect of treatment ($P=0.760$). The interaction between treatment and set also was not statistically different ($P=0.2413$). This analysis indicated that F_{min} decay and isometric force decay during the protocol were similar for the stretch–shortening group and isometric control group.

Discussion

Skeletal muscle experiences damage during repeated eccentric contractions. It is accepted that changes in mechanical behavior are the best means to evaluate the magnitude and time course of muscle injury in animals and humans (Warren et al. 1999). Our results indicate that the isometric forces for both the stretch–shortening and control groups exhibited a substantial reduction immediately after exposure to the protocol. However, after a break of 48 h, the isometric force of the stretch–shortening group remained almost unchanged, while the isometric force from the control group recovered almost completely (Fig. 3). Assuming that depression of the isometric force could be induced by both fatigue and tissue damage, the former could be recovered in a short period (e.g., several hours), while the latter would not. Our results suggest that repeated stretch–shortening cycles induced tissue damage while repeated isometric contractions induced fatigue that recovered in a short period of time.

We also surmise that the control group which consisted of only isometric contractions was an accurate

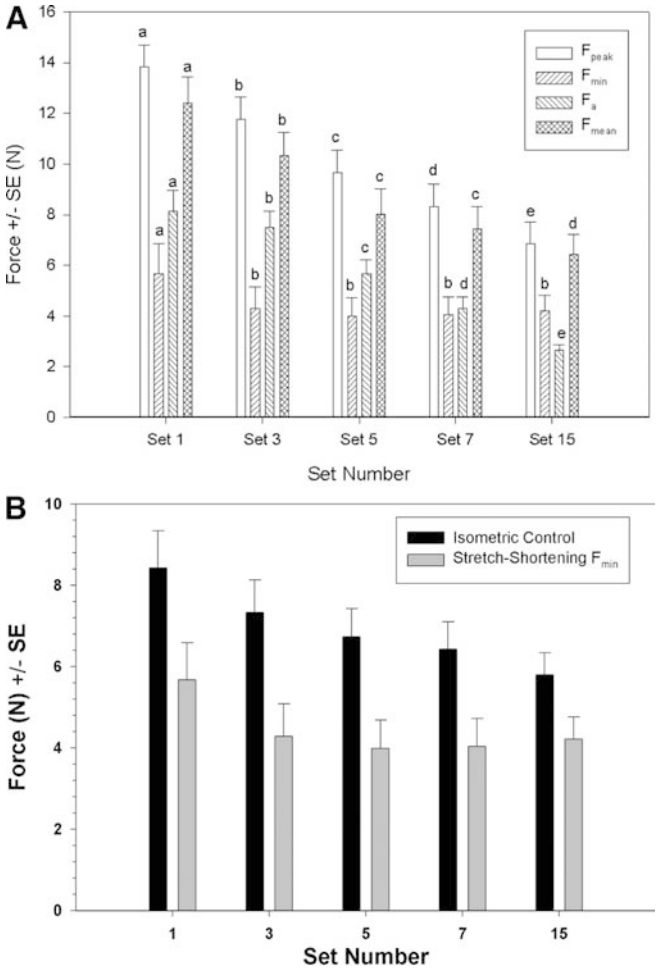

Fig. 7A, B Variations of the characterized force parameters of the muscles. **A** The F_{min}, F_{mean}, F_{peak}, and F_a, as a function of the number of cycles. Statistical difference at the 0.05 level for the each of the force parameters at different sets is denoted by a different letter. **B** The F_{min} values were compared to isometric forces in the control protocol which corresponded to the same time point in each set. Statistical analyses indicated that there was no significant interaction between treatment and set ($P = 0.0940$)

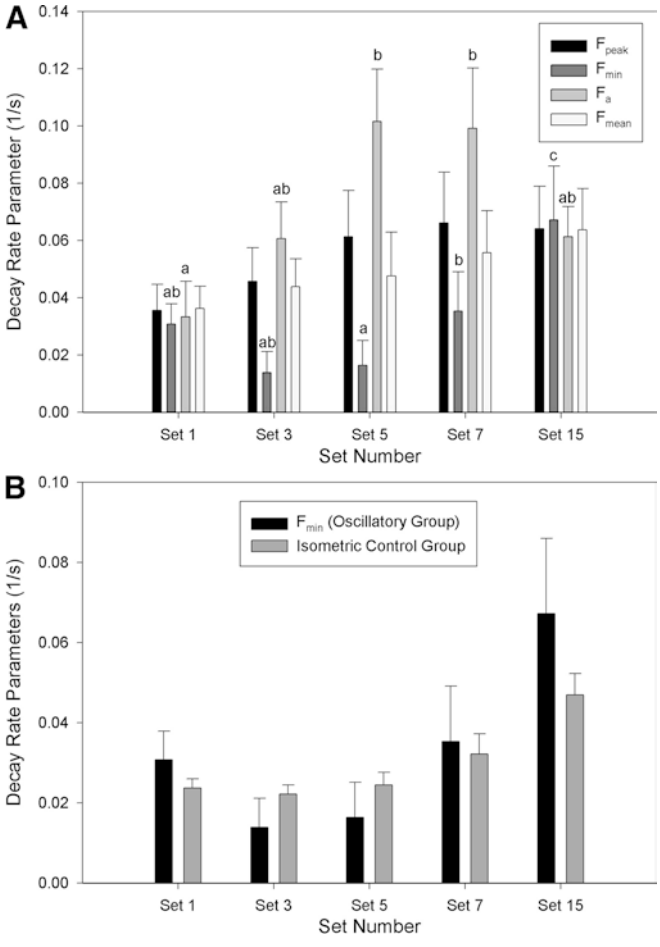

Fig. 8A, B Force decay parameters of the dorsi flexor muscle group of rats. **A** The variations of the force decay parameters during stretch–shortening cycles. Statistical difference at the 0.05 level for the each of the decay rate parameters at different sets is denoted by a different letter. **B** The decay of the minimum force in the injury (stretch–shortening cycle) group compared with that of the isometric force in the control (isometric contraction) group

indicator of the metabolic demand of the stretch–shortening protocol which contained eccentric muscle actions (Armstrong 1984; Lieber et al. 1991; Willems and Stauber 2000b). This hypothesis was also supported by the studies of Hesselink et al. (1998), who used similar stimulation durations as the present study and indicated that muscle glycogen stores and high energy phosphates in the rat tibialis anterior muscle exhibited a similar decrement after multiple eccentric and isometric contractions.

In our study, the variations in the dynamic force response during the protocol were evaluated by comparing the change in force parameters between sets and the decay of those parameters within each set. The force drop between sets was compared using the force values for the first repetition of each set. The first repetition point was chosen since it was least affected by the fatigue between sets. The force decay between the sets indicated the rate at which force was dropping throughout the experimental protocol. The force decay during each set (first to tenth repetition) was used to evaluate the dorsi flexors ability to maintain force for the 2.8 s activation time.

Up to set 5, the stretch–shortening parameters F_{peak}, F_{min}, F_{mean}, and F_a exhibited similar decrements (Figs6, 7A). However, after set 5, the F_{peak}, F_{mean}, and F_a exhibited significant decrements, while F_{min} exhibited no additional decrement and approached steady-state.

The α value for F_a increased over the first half of the sets peaking at sets 5 and 7 (Fig. 8A). This result indicated that the eccentric performance of the dorsi flexors declined more during each successive set up to set 7. As F_a exhibited its maximum decay, the decay in F_{min} started to increase, which is most likely attributed to progressive muscle fatigue. It is likely that the majority of muscle damage occurred within the first half of the experimental sets when the muscle was able to maintain a high force. This was supported by a large decay in minimum force

for sets 7–15 and the relatively large α values of F_a at sets 5–7. In addition, the pathology score for myofiber degeneration and necrosis, while numerically higher at 15 sets, was not statistically distinguishable from myofiber degeneration and necrosis observed after set 7 (Fig. 5A). The stretch–shortening protocol did indeed produce myofiber damage in the tibialis anterior 48 h after 150 stretch–shortening cycles, as indicated by myofiber degeneration and necrosis with associated inflammation (Figs 4D, 5C, D). The isometric protocol was not associated with morphologic evidence of myofiber degeneration or necrosis, although limited inflammation was associated with the procedure (Fig. 5C, D).

The isometric control group exhibited a drop in force from the first to third set then gradually decreased with each set up to a total decrement of approximately 25% of its initial value which was similar to the total decrement in F_{min} values (Fig. 7B). In addition, the F_{min} and isometric control group α values were similar during the 15 set protocol. These results suggest that the F_{min} values and isometric control group forces exhibited similar behavior between sets and within sets during the protocol which suggests that the drop in F_{min} within the stretch–shortening group was associated with the fatigue between sets and the F_{min} α value was associated with the fatigue within sets.

In summary, the investigation of muscle response during controlled dynamic movements provided valuable information about changes in isometric and eccentric/concentric muscle performance during dynamic perturbations. The results from this protocol suggest that changes in eccentric performance above the isometric baseline (derived from changes in F_a) may be the best indicator of muscle damage. The results suggest that damage occurs between sets 5 and 7 due to the high decay rate in F_a during those sets. The results also predict that damage should not occur in previous sets. This prediction was supported by subsequent findings of statistically significant myofiber degeneration and necrosis after exposure to 70 stretch–shortening cycles but not after 30 stretch–shortening cycles (Fig. 5A). Specifically, after 30 cycles, two rats had no evidence of myofiber damage while four rats had multiple foci of degeneration and necrosis, which never coalesced and were considered minimal to mild in severity. In contrast, after 70 stretch–shortening cycles, degeneration and necrosis was seen in all rats with a severity from mild to marked distributed in multiple foci which were coalescent in four of the six rats. In addition, the analysis of real-time changes in F_{min} was a good indicator of the progression of fatigue during the protocol. Quantifying the change in muscle performance under controlled dynamic conditions may provide useful information about injury susceptibility, fatigue rates, and effects of modulating factors such as training, disuse, and aging on performance and injury response.

Acknowledgements The authors would like to thank Vincent Kish for fabrication of the dynamometer, Sam Stone for fabrication of computer/equipment interface hardware, and the discussions with Drs. Walter Herzog, Aaron Schopper, and Steve Alway who helped to improve the manuscript.

References

Armstrong RB (1984) Mechanism of exercise-induced delayed onset muscular soreness: a brief review. Med Sci Sports Exerc 16:529–538

Avela J, Komi PV (1998) Reduced stretch reflex sensitivity and muscle stiffness after long-lasting stretch–shortening cycle exercise in humans. Eur J Appl Physiol 78:403–410

Benn C, Forman K, Mathewson D, Tapply M, Tiskus S, Whang K, Blanpied P (1998) The effects of serial stretch loading on stretch work and stretch–shorten cycle performance in the knee musculature. J Orthop Sports Phys Ther 27:412–422

Benz R, Friden J, Lieber R (1998) Simultaneous stiffness and force measurements reveal subtle injury to rabbit soleus muscles. Mol Cell Biochem 179:147–158

Carter WO, Bull C, Bortolon E, Yang L, Jesmok GJ, Gundel RH (1998) A murine skeletal muscle ischemia-reperfusion injury model: differential pathology in BALB/c and DBA/2 N mice. J Appl Physiol 85:1676–1683

Clarkson PM, Newham DJ (1995) Associations between muscle soreness, damage, and fatigue. Adv Exp Med Biol 384:57–69

Cutlip RG, Stauber W, Willison R, McIntosh T, Means K (1997) A dynamometer for rat plantar flexor muscle in vivo. Med Biol Eng Comput 35:540–543

Faulkner JA, Jones DA, Round JM (1981) Injury to skeletal muscles of mice by forced lengthening during contractions. Q J Exp Physiol 74:661–670

Friden J, Sjostrom M, Ekblom B (1981) A morphological study of delayed muscle soreness. Experientia 37:506–507

Friden J, Seger J, Sjostrom M, Ekblom B (1983) Adaptive response in human skeletal muscle subjected to prolonged eccentric training. Int J Sports Med 3:177–183

Helliwell TR (1999) Muscle. Part 2. Muscle damage: its causes and investigation. Curr Orthop 13:131–143

Hesselink MK, Kuipers H, Geurten P, Straaten H van (1996) Structural muscle damage and muscle strength after incremental number of isometric and forced lengthening contractions. J Muscle Res Cell Motil 17:335–341

Hesselink M, Kuipers H, Keizer H, Drost M, Vusse G van der (1998) Acute and sustained effects of isometric and lengthening muscle contractions on high-energy phosphates and glycogen metabolism in rat tibialis anterior muscle. J Muscle Res Cell Motil 19:373–380

Hubbs AF, Battelli LA, Goldsmith WT, Porter DW, Frazer D, Friend S, Schwegler-Berry D, Mercer RR, Reynolds JS, Grote A, Castranova V, Kullman G, Fedan JS, Dowdy J, Jones WG (2002) Necrosis of nasal and airway epithelium in rats inhaling vapors of artificial butter flavoring. Toxicol Appl Pharmacol 185:128–135

Ingalls CP, Warren GL, Williams CW, Ward JH, Armstrong RB (1998) E–C coupling failure in mouse EDL muscle after in vivo eccentric contractions. J Appl Physiol 85:2555–2564

Josephson RK (1985) The mechanical power output of a tettigoniid wing muscle during singing and flight. J Exp Physiol 117:357–368

Koh TJ, Herzog W (1998) Eccentric training does not increase sarcomere number in rabbit dorsiflexor muscles. J Biomech 31:499–501

Komulainen J, Takala TE, Kuipers H, Hesselink MK (1998) The disruption of myofibre structures in rat skeletal muscle after forced lengthening contractions. Pflugers Arch 436:735–741

Kyrolainen H, Takala TE, Komi PV (1998) Muscle damage induced by stretch–shortening cycle exercise. Med Sci Sports Exerc 30:415–420

Lieber RL, Woodburn TM, Friden J (1991) Muscle damage induced by eccentric contractions of 25% strain. J Appl Physiol 70:2498–2507

Lieber RL, Thornell LE, Friden J (1996) Muscle cytoskeletal disruption occurs within the first 15 min of cyclic eccentric contraction. J Appl Physiol 80:278–284

Lowe DA, Warren GL, Ingalls CP, Boorstein DB, Armstrong RB (1995) Muscle function and protein metabolism after initiation of eccentric contraction-induced injury. J Appl Physiol 79:1260–1270

McCully KK, Faulkner JA (1986) Characteristics of lengthening contractions associated with injury to skeletal muscle fibers. J Appl Physiol 61:293–299

Morgan DL, Allen DG (1999) Early events in stretch-induced muscle damage. J Appl Physiol 87:2007–2015

Newham DJ, McPhail G, Mills KR, Edwards RH (1983) Ultrastructural changes after concentric and eccentric contractions of human muscle. J Neurol Sci 61:109–122

Newham DJ, Jones DA, Clarkson PM (1987) Repeated high-force eccentric exercise: effects on muscle pain and damage. J Appl Physiol 63:1381–1386

Patel TJ, Cuizon D, Mathieu-Costello O, Friden J, Lieber RL (1998) Increased oxidative capacity does not protect skeletal muscle fibers from eccentric contraction-induced injury. Am J Physiol 274:R1300–R1308

Stevens ED (1996) Effect of phase of stimulation on acute damage caused by eccentric contractions in mouse soleus muscle. J Appl Physiol 80:1958–1962

Warren GL, Hayes DA, Lowe DA, Armstrong RB (1993) Mechanical factors in the initiation of eccentric contraction-induced injury in rat soleus muscle. J Physiol (Lond) 464:457–475

Warren GL, Williams JH, Ward CW, Matoba H, Ingalls CP, Hermann KM, Armstrong RB (1996) Decreased contraction economy in mouse edl muscle injured by eccentric contractions. J Appl Physiol 81:2555–2564

Warren G, Lowe D, Armstrong R (1999) Measurement tools used in the study of eccentric contraction-induced injury. Sports Med 27:43–56

Willems ME, Stauber WT (1999) Isometric and concentric performance of electrically stimulated ankle plantar flexor muscles in intact rat. Exp Physiol 84:379–389

Willems ME, Stauber WT (2000a) Force output during and following active stretches of rat plantar flexor muscles: effect of velocity of ankle rotation. J Biomech 33:1035–1038

Willems ME, Stauber WT (2000b) Performance of plantar flexor muscles with eccentric and isometric contractions in intact rats. Med Sci Sports Exerc 32:1293–1299

Willems ME, Stauber WT (2001) Force deficits after repeated stretches of activated skeletal muscles in female and male rats. Acta Physiol Scand 172:63–67